

**Double ionization of helium by intense near-infrared and VUV laser pulses**Shaohao Chen,<sup>1</sup> Camilo Ruiz,<sup>2</sup> and Andreas Becker<sup>1</sup><sup>1</sup>*JILA and Department of Physics, University of Colorado, Boulder, Colorado 80309-0440, USA*<sup>2</sup>*Centro de Laseres Pulsados Ultraintensos Ultracortos (CLPU), Plaza de la Merced s/n, Salamanca E-37006, Spain*

(Received 12 May 2010; published 23 September 2010)

We investigate the dynamics of double ionization of He atom by an intense near-infrared and an attosecond vacuum ultraviolet (VUV) laser pulse, which are either applied in sequence or at the same time. To this end we solve the time-dependent Schrödinger equation for a two-electron model atom interacting with the two fields. We compare the double-ionization yields and probability density distributions, with and without the application of the attosecond pulse, for the different scenarios. The results of our numerical simulations show how ionization or excitation of the neutral atom by a preceding or simultaneously applied VUV pulse affects the double-ionization dynamics driven by the near-infrared laser pulse. The findings provide insights regarding the question if attosecond technology can be used to temporally resolve mechanisms of correlated emission of electrons in a strong laser field.

DOI: [10.1103/PhysRevA.82.033426](https://doi.org/10.1103/PhysRevA.82.033426)

PACS number(s): 32.80.Rm, 32.80.Wr

**I. INTRODUCTION**

Double ionization of helium provides fundamental insights into the role of electron-electron correlation, since it is the simplest system in which this interaction can be studied. It serves as a prototype example for understanding electron correlation effects, which are relevant in larger systems such as molecules and clusters as well. The advent of subfemtosecond laser technology with the generation of attosecond pulses from the vacuum ultraviolet (VUV) up to the extreme ultraviolet (XUV) wavelength regime (for reviews, see, e.g., Refs. [1,2]) has opened new perspectives toward the observation of the correlated electron dynamics in double ionization of atoms and molecules. For example, few-photon double ionization can now be observed using higher-order harmonics [3,4] or intense light generated by free-electron lasers [5,6]. In particular, the two-photon process has become a subject of intense theoretical studies (e.g., Refs. [4,7–18]). On the other hand, the attosecond pulse duration can be used to temporally resolve subcycle electron dynamics in processes driven by an intense near-infrared (IR) field. This concept has been applied to probe the time scale of strong-field (tunnel) ionization of atoms [19]. It is, however, unclear whether this technique can be used to reveal dynamical electron correlation effects in the double-ionization process, induced by an external near-infrared laser field, as well.

In the absence of electron correlation one would expect that strong-field double ionization proceeds via a sequential mechanism, in which the electrons are emitted one after the other by subsequent independent absorption of photons from the external field. It is, however, well known, that double-ionization yields at near-infrared laser wavelengths and intensities between  $10^{13}$  and  $10^{15}$  W/cm<sup>2</sup> exceed the expectations based on the sequential mechanism by many orders of magnitude [20,21]. These observations provided the evidence of an effective nonsequential mechanism mediated via electron correlation. A common interpretation of the nonsequential process has been reached over the past decade (for a review, see, e.g., Ref. [22]). The correlated electron emission comprises two pathways via the rescattering picture [23–25]. According to this picture, an initially field

ionized electron is driven back to the parent ion and either ionizes [23] or excites [28–30] the residual ion via the electron correlation interaction. In the case of excitation, which is known as the recollision-induced excitation plus subsequent field ionization (RESI) process, the excited ionic states are likely to decay within less than a femtosecond between the instant of excitation (near a zero of the field) and the next field maximum (e.g., Refs. [31,32]). Attosecond technology appears to be the appropriate tool to probe this ultrafast dynamics in the excited states of the ion.

As a step toward this goal, below we make an effort to gain insights in the dynamics of a two-electron atom interacting with an attosecond VUV pulse and an intense near-infrared pulse, which are either applied in sequence or at the same time. To this end, we have performed numerical simulations of the correlated electron emission from helium atom in the combined fields. For our calculations we have used a two-electron model, in which the center-of-mass motion of the two electrons is restricted along the polarization direction of the external fields [33]. It has been shown previously [31–34] that despite the reduction in dimensions the model can provide useful qualitative insights into the dynamics of the correlated electron emission.

The remainder of the article is organized as follows: In the next section we investigate the parameter regimes (intensity, wavelength, and pulse duration) of the VUV probe pulse by studying the ionization yields from scaled one-electron atoms. In Sec. III we outline the two-electron model for the helium atom and use it in Sec. IV to analyze single and double ionization of the atom by separated, nonoverlapping IR and VUV pulses. Then, in Sec. V, we present our results for an application of the VUV pulse in the presence of the IR pulse. The paper ends with concluding remarks. We use hartree atomic units ( $e = m = \hbar = 1$ ) unless mentioned otherwise.

**II. PARAMETER REGIMES OF THE VUV PROBE PULSE**

In this section we will obtain a range of parameters for the VUV probe pulse which should be favorable for a potential future study of the excited state population in the He<sup>+</sup> ion. We consider the unperturbed system for this purpose. In order

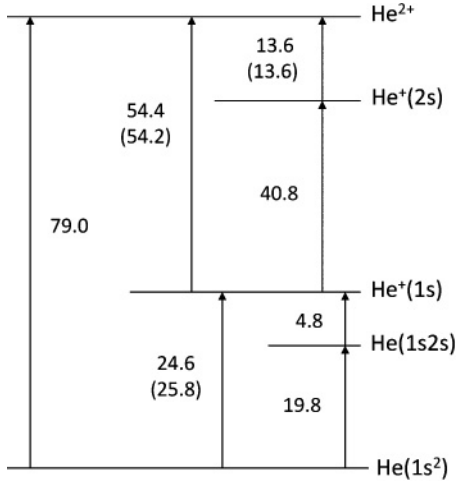


FIG. 1. Energy levels of He and He<sup>+</sup> (in eV). The energies outside the brackets are experimental data [35] or accurate theoretical results, while those in the brackets are obtained by the 3D model, as described in Sec. III.

to maximize the ionization (probe) yields from all the excited states in He<sup>+</sup>, we should require that those processes are induced by the absorption of one photon, i.e.,  $\hbar\Omega_{\text{VUV}} > 13.6$  eV (cf. Fig. 1). On the other hand,  $\hbar\Omega_{\text{VUV}}$  should be smaller than 19.8 eV such that ionization and excitation from the ground states of the neutral atom and the ion proceed via two- (or higher order) photon absorption only. In this case, we expect the corresponding yields to be weak as compared to the yields from the excited ionic states. These two requirements restrict the photon energy to a small regime, for example, the ninth and eleventh harmonics of a Ti:sapphire laser pulse operating at about 800 nm. For the actual calculations we have used the harmonics of a driver pulse at about 800 nm (ninth harmonic: 89 nm or 13.9 eV, eleventh harmonic: 73 nm or 17 eV).

To verify our expectations and select the intensity and pulse duration of the VUV pulse, we compare the total ionization probabilities for the interaction of a VUV pulse with the He atom in its ground state as well as the He<sup>+</sup> ion in its ground and first excited state, respectively. To this end, we have performed numerical calculations of the time-dependent Schrödinger equation for scaled one-electron atoms with effective nuclear charges  $Z_{\text{eff}}$  interacting with an external field. The corresponding Hamiltonian is given by (in dipole approximation and velocity gauge)

$$H(\rho, z, t) = \frac{p_z^2}{2} + \frac{p_\rho^2}{2} + \frac{Z_{\text{eff}}}{\sqrt{\rho^2 + z^2 + a^2}} - \frac{p_z A(t)}{c}, \quad (1)$$

where  $(z, \rho)$  and  $(p_z, p_\rho)$  are the coordinate and momentum of the electron,  $a^2 = 0.001$  is a soft-core Coulomb parameter, and  $A(t)$  is the vector potential of the linearly polarized VUV laser field. The effective charge  $Z_{\text{eff}}$  has been chosen to be equal to 1, 1.38, and 2. We have chosen these specific values such that the ground-state energies of the one-electron atoms correspond to the energy values in the 3D two-electron model used for the full two-electron calculations below (cf. Table I). In case of the two-electron model it is not possible to reproduce all the energy levels of the real He atom. In the present calculations we have chosen to reproduce the ionization potential

TABLE I. Ionization thresholds  $I_p$  (in eV) of the scaled one-electron atoms with effective nuclear charge  $Z_{\text{eff}}$  and minimum number of photons of energy  $E$ ,  $N_{\text{min}}[E] = \text{Int}(I_p/E)$ , needed to be absorbed to overcome the ionization threshold.

$Z_{\text{eff}}$	$I_p$	Corresponds to	$N_{\text{min}}(13.9 \text{ eV})$	$N_{\text{min}}(17 \text{ eV})$
1	13.6	He <sup>+</sup> (2s)	1	1
1.38	25.8	He(1s <sup>2</sup> )	2	2
2	54.2	He <sup>+</sup> (1s)	4	3

( $I_p = 54.2$  eV) and the excitation potential to the 2s state (13.6 eV) of the He<sup>+</sup> ion, while the ionization potential of the He atom ( $I_p = 25.8$  eV in the present model) varies slightly from the values in the real He atom. The energy values of the 3D model are shown in Fig. 1 (values in brackets) along with the values of the real He atom.

The Schrödinger equation has been solved on a grid using the Crank-Nicolson method, and the respective ground states are obtained by imaginary time propagation without the external field. The grid parameters were  $N_\rho = 500$ ,  $N_z = 1200$ , and  $\Delta_\rho = \Delta_z = 0.1$  a.u. and the time step  $\Delta t = 0.02$  a.u. The outgoing part of the wave function, which corresponds to the ionization of the atom, was absorbed by applying a  $\cos^2$  mask function at the boundaries of the grid. The corresponding probability, which we define as the total ionization probability (TIP), was monitored until the results converged.

The results for the TIPs as a function of the peak intensity  $I$  for (a) a ten-cycle pulse at 73 nm, (b) a two-cycle pulse at 73 nm, and (c) a two-cycle pulse at 89 nm are shown in Fig. 2. The ten-cycle pulse (1.2 fs) is used for the sake of comparison only, since its duration is actually too long for a study of the subcycle dynamics in the excited state of the He<sup>+</sup> ion. For this long pulse [Fig. 2(a)] the TIPs are approximately proportional to  $I$ ,  $I^2$ , and  $I^3$  for  $Z_{\text{eff}} = 1, 1.38$ , and 2, respectively, until saturation of the individual process is reached at high intensities. These results indicate that, as expected from energy considerations (cf. Table I), one, two, and three 17-eV photons are absorbed to ionize the respective model atoms. Due to its narrow bandwidth (0.5 eV) the pulse is not in resonance with the first excited state of the scaled one-electron atoms with  $Z_{\text{eff}} = 1.38$  and 2.

For the shorter pulse at the same wavelength [Fig. 2(b)] the results show a similar trend. However, for  $Z_{\text{eff}} = 1.38$  the TIP is approximately proportional to  $I^1$  rather than  $I^2$  in the low-intensity region. This indicates a resonant two-photon (1+1 photon) process via the first excited state, which is possible due to the large bandwidth of the pulse (2.7 eV). At higher intensities, the first excited state is shifted to higher energies in the presence of the strong field and cannot be further populated during the ionization process. On the other hand, the bandwidth of the two-cycle, 89-nm (13.9 eV) pulse is about 2.2 eV and the first excited state of the model He atom ( $Z_{\text{eff}} = 1.38$ ) is outside of this bandwidth. Correspondingly in this case [Fig. 2(c)] the scaling of the TIP ( $\propto I^2$ ) indicates a nonresonant two-photon transition.

We may therefore expect that for a two-cycle pulse (at the wavelengths considered above) large ionization probabilities from the excited states of He<sup>+</sup> and relatively small ionization probabilities from the ground state of He in the intensity regime

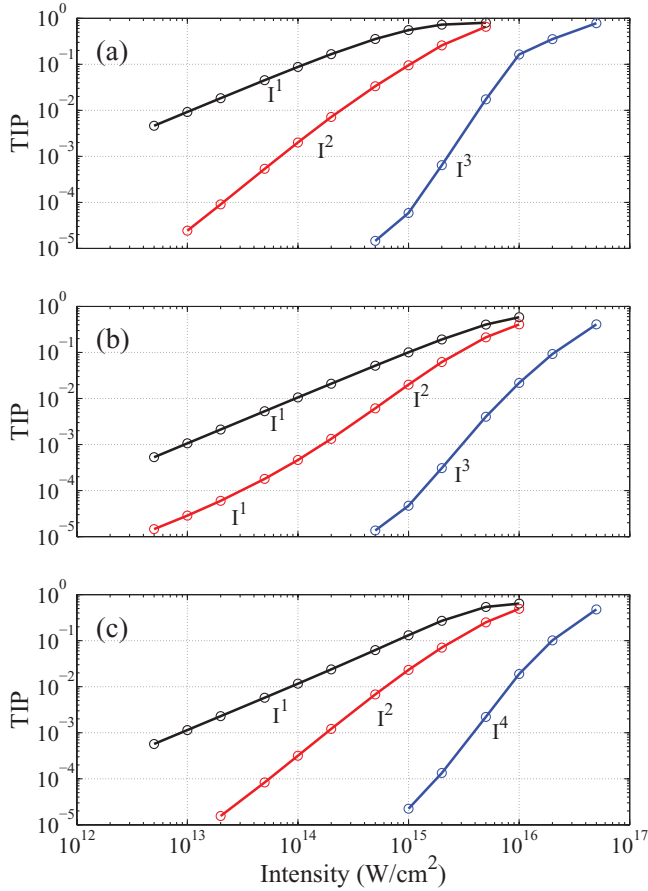


FIG. 2. (Color online) TIPs as a function of peak intensity due to the interaction of a scaled one-electron atom with  $Z_{\text{eff}} = 1$  (black line), 1.38 (red line), and 2 (blue line) with (a) a ten-cycle, 73-nm pulse, (b) a two-cycle, 73-nm, and (c) a two-cycle, 89-nm intense laser pulse.

around  $10^{14}$  W/cm<sup>2</sup> are generated. For the actual simulations of the double-ionization process in helium atom we have chosen a two-cycle pulse at 73 nm with a peak intensity of  $10^{14}$  W/cm<sup>2</sup>.

### III. TWO-ELECTRON MODEL

In order to analyze the interaction of He atom with a near-infrared and a VUV pulse, we make use of a two-electron model in which the center-of-mass motion of the two electrons is restricted to the polarization direction of the two lasers. We therefore assume that both laser pulses are linearly polarized in the same direction. The corresponding Hamiltonian can be expressed as [33],

$$\begin{aligned}
 H(Z, \rho, z, t) = & \frac{P_Z^2}{4} + p_\rho^2 + p_z^2 + \frac{1}{\sqrt{\rho^2 + z^2}} \\
 & - \frac{2}{\sqrt{\rho^2/4 + (Z + z/2)^2 + a^2}} \\
 & - \frac{2}{\sqrt{\rho^2/4 + (Z - z/2)^2 + a^2}} \\
 & - \frac{P_Z [A_1(t) + A_2(t)]}{c}, \quad (2)
 \end{aligned}$$

where  $Z$  and  $P_Z$  are the center-of-mass coordinate and momentum in the field direction,  $z, \rho$  and  $p_z, p_\rho$  are the components of the relative electron coordinates and momenta in polarization direction and perpendicular to it.  $a^2 = 0.135$  is a soft-core Coulomb parameter and  $A_i(t)$  is the vector potential of the  $i$ th laser field. As outlined before, in the present model we cannot reproduce all energy values and ionization potentials of the real He atom. We have chosen the soft-core Coulomb parameter such that the ionization potential of the model He<sup>+</sup> ion corresponds to that of the real system (cf. Fig. 1). We have solved the corresponding time-dependent Schrödinger equation for a He atom, which is initially in its ground state, using the Crank-Nicolson method. The ground-state wave function of the He atom is obtained by imaginary time propagation without the field.

We have analyzed the ionization dynamics by calculating single- and double-ionization probabilities, as well as probability distributions as a function of time. For the calculations of the total probabilities at different intensities we have varied the grid size such that the dimensions correspond to about 1.5 times the amplitude of the classical motion of the electron in the field in each case. A cos<sup>2</sup> mask function has been used at the boundaries to absorb the outgoing parts of the wave functions, which are, however, stored for the calculation the ionization probabilities. Single- and double-ionization probabilities have been determined by partitioning the grid in different regions [33,34]:

$$\begin{aligned}
 r_1 = \sqrt{\rho^2/4 + (Z + z/2)^2} < 12 \text{ a.u.} \quad \text{and} \\
 r_2 = \sqrt{\rho^2/4 + (Z - z/2)^2} < 12 \text{ a.u.}, \quad \text{He atom,} \\
 r_1 < 6 \text{ a.u.} \quad \text{and} \quad r_2 > 12 \text{ a.u.}, \quad \text{or} \quad (3) \\
 r_1 > 12 \text{ a.u.} \quad \text{and} \quad r_2 < 6 \text{ a.u.}, \quad \text{He}^+ \text{ ion,} \\
 \text{rest of space,} \quad \text{He}^{2+} \text{ ion.}
 \end{aligned}$$

For the calculations of the probability distributions a larger grid with  $N_\rho = 120$ ,  $N_z = 1200$ ,  $N_Z = 600$  has been used to retain the wave function on the grid. In each of the calculations we have used a grid spacing of  $\Delta\rho = \Delta z = \Delta Z = 0.3$  a.u. and a time step of 0.05 a.u.

### IV. DOUBLE IONIZATION OF HELIUM BY A SEQUENCE OF NEAR-INFRARED AND VUV PULSES

First, we have calculated the single- and double-ionization probabilities as a function of peak intensity for interaction of the (model) He atom with either a four-cycle near-infrared (IR) pulse at 800 nm (1.55 eV) or a two-cycle VUV pulse at 73 nm (17 eV) alone. The results are plotted as a function of peak intensity  $I$  in Fig. 3. In agreement with our previous results [Fig. 2(b)], we find that over the whole intensity regime investigated the single-ionization probability due to the interaction with the VUV pulse is proportional to  $I^2$ , as expected for a two-photon absorption process. Double ionization due to the VUV pulse cannot be detected in our numerical calculations for intensities below  $2 \times 10^{14}$  W/cm<sup>2</sup>. For the IR pulse, the single- and double-ionization probabilities increase quickly beyond the thresholds of  $4 \times 10^{14}$  W/cm<sup>2</sup> and  $5 \times 10^{14}$  W/cm<sup>2</sup>, respectively. We note that the predictions for the ratio of double-to-single ionization yield at 800 nm is rather

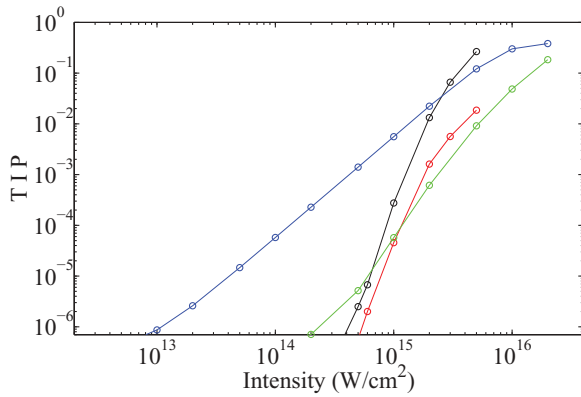


FIG. 3. (Color online) Total single- (SI) and double-ionization (DI) probabilities as a function of peak intensity. From left to right at low TIPs: (blue line) SI probabilities induced by a VUV pulse at 73 nm; (green line) DI probabilities induced by a VUV pulse at 73 nm; (black line) SI probabilities induced by a IR pulse at 800 nm; (red line) DI probabilities induced by a IR pulse at 800 nm.

large within the present model. This indicates that the electron correlation interaction is too strong in the model. This will, however, not influence the qualitative conclusions from the present calculations.

In view of these results we have chosen for our further analysis of the double-ionization dynamics in the combined fields a VUV peak intensity of  $10^{14}$  W/cm<sup>2</sup> and an IR peak intensity of  $5 \times 10^{14}$  W/cm<sup>2</sup> which are both below the (detection) threshold intensities for double ionization for interaction with just one of these pulses. Thus any double-ionization probability, observed in the results presented below, has to be due to the interaction of the He atom with *both* pulses.

Next, we consider the application of both pulses but with a time delay of about 2.4 fs. Single- and double-ionization probabilities as a function of time are obtained for both cases, namely that the VUV pulse follows (Fig. 4) or precedes (Fig. 5) the IR pulse.

If the VUV pulse follows the IR pulse, the single-ionization probability (Fig. 4) rises at the maxima of the IR field as well as at the main field maximum of the VUV pulse. The short delays in the rise of probabilities as compared to the position of the maxima are due to the fact that we define the ionization probabilities by partitioning the grid and the singly ionized part of the wave function has to reach the corresponding region before it is accounted for single ionization. We note that the VUV pulse may ionize the He atom from its ground state or from excited states, which are pumped during the interaction with the IR field. There is no double-ionization signal found in the calculations.

In the case where the VUV pulse precedes the IR pulse (Fig. 5), the single-ionization probability (solid line) first increases rapidly due to the interaction with the VUV pulse. Next, we see two further increases during the interaction with the IR pulse. In contrast to the case where the IR precedes the VUV pulse (Fig. 4) these strong rises in the signal, however, occur during the second and third (rather weak) field maxima but not during the main maxima of the pulse. We interpret this result as due to single ionization from excited neutral states which are pumped during the preceding VUV pulse. Due to

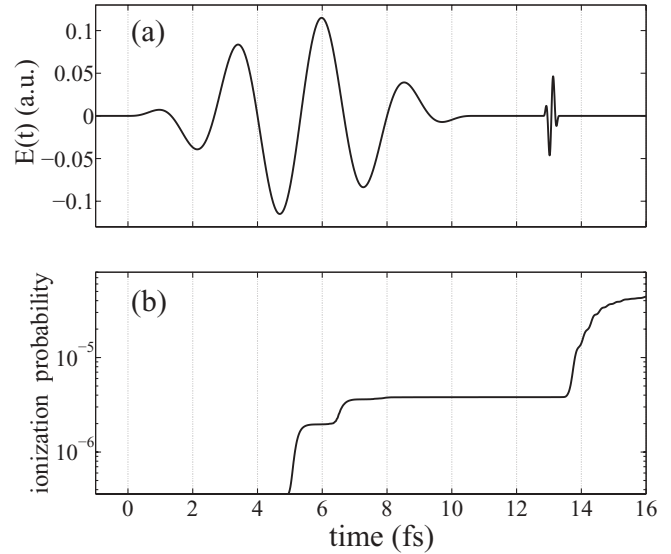


FIG. 4. Interaction of the (model) He atom with a sequence of IR pulse followed by an attosecond VUV pulse. (a) Field amplitude as a function of time. (b) Single ionization probabilities as a function of time. There is no double-ionization signal found in our calculation. IR pulse parameters: 800 nm,  $5 \times 10^{14}$  W/cm<sup>2</sup>, four cycles. VUV pulse parameters: 73 nm,  $10^{14}$  W/cm<sup>2</sup>, two cycles.

the depletion of the excited state population during the second and third field maxima, there is no single ionization at the following larger field maxima.

We also observe a strong double-ionization signal (dashed line) in this case. Since there is no double ionization from the ground state of the He atom induced by the IR alone (cf. Fig. 3), this contribution has to be related to the presence of the preceding VUV pulse as well. It is therefore likely that the excited states in the neutral atom, pumped by the VUV pulse, and the rescattering of the electron emitted from these states are the origin of the double-ionization signal.

We have also evaluated the probability density in the Z-z plane by modulo squaring the wave function and integrating

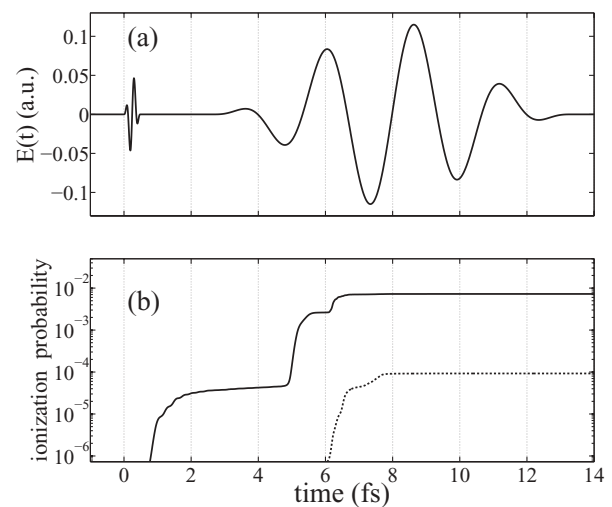


FIG. 5. Same as Fig. 4, but for a sequence of an attosecond VUV pulse followed by an IR pulse. In (b), solid line for single ionization and dashed line for double ionization.

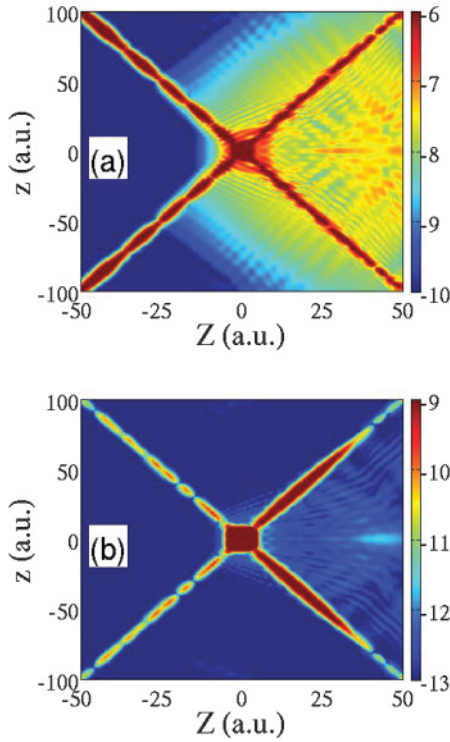


FIG. 6. (Color online) Probability distributions in the  $Z$ - $z$  plane taken at the middle of the IR pulse (at about 8 fs) (a) with and (b) without application of the VUV pulse.

the result over the component ( $\rho$ ) of the relative electron coordinate perpendicular to the polarization direction. Figure 6 shows the probability density in the middle of the IR pulse at about 8 fs. We compare the densities for the cases with [Fig. 6(a)] and without [Fig. 6(b)] preceding VUV pulse. In these plots the probability density corresponding to the neutral He atom is found in the middle of the plot around  $Z \approx 0$  and  $z \approx 0$ , the single-ionization probability density is along the diagonals, while the double-ionization probability density is found in the four triangles separated by the diagonals. Comparing the probability density distributions, the enhancement in both the SI and DI yields in the case where the VUV pulse is applied is obvious. Please note that the color scale in the two panels is different, indicating that the signals are about three orders of magnitude larger in Fig. 6(a) than in Fig. 6(b). In the case of the preceding VUV pulse [Fig. 6(a)] the double-ionization density mainly appears in the right triangle, which is in agreement with the interpretation of a rescattering event.

## V. DOUBLE IONIZATION OF HELIUM IN THE COMBINED FIELDS

Next, we investigate single and double ionization by the combined fields of the VUV pulse and the IR pulse. In Fig. 7 we present single- [Fig. 7(b)] and double-ionization probabilities [Fig. 7(c)] obtained for application of the VUV pulse (two-cycle, 73-nm attosecond pulse,  $10^{14}$  W/cm<sup>2</sup>) at different time instants during the four-cycle, 800-nm pulse ( $5.3$  fs,  $5 \times 10^{14}$  W/cm<sup>2</sup>). The time delays [(1), (2), and (3)] considered in the present calculations can be read from the

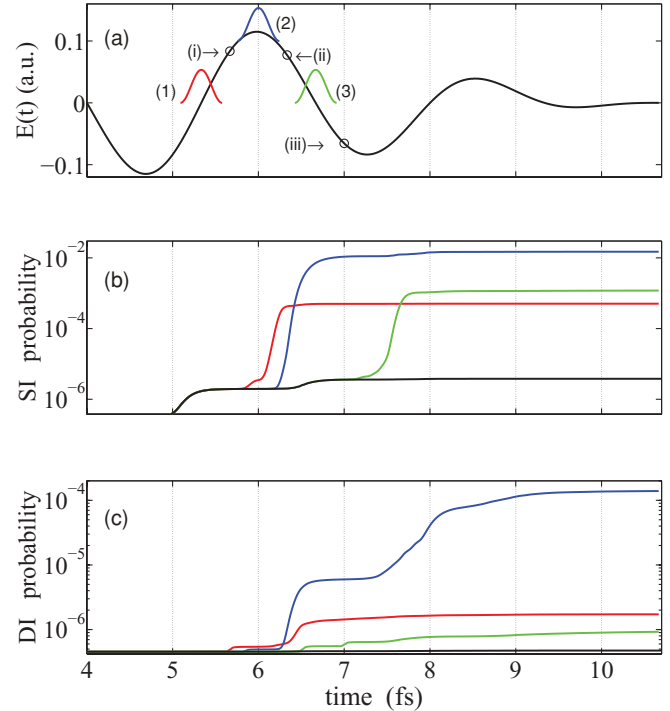


FIG. 7. (Color online) (a) IR field amplitude as a function of time. The VUV pulse is applied at different time instants (1)  $t = 2T$ , (2)  $t = 9T/4$ , and (3)  $t = 5T/2$  in the presence of the IR pulse. Single- (b) and double-ionization (c) probabilities as a function of time. (Black line) Without VUV pulse. (Red, blue, and green lines) Application of the VUV pulse at time instants (1), (2), and (3), respectively. The corresponding probability distributions at the time instants (i)  $t = 17T/8$ , (ii)  $t = 19T/8$ , and (iii)  $t = 21T/8$  are shown in the Figs. 8–10 below.

sketch of the field amplitudes in Fig. 7(a). Whenever the VUV pulse is applied we observe a strong increase in the single- and double-ionization signal, as compared to the results obtained for the IR pulse alone (black lines).

The enhancement in the single-ionization signal can be explained in each case as due to two-photon ionization by the VUV pulse. The double-ionization signals reveal, however, a more complex dynamics. For each of the three time instants, at which the VUV pulse is applied, we observe an increase in the double-ionization signal during the interaction with the VUV pulse. This increase is small when the VUV pulse is applied near a zero of the IR field [time instants (i) and (iii), red and green lines, respectively]. But it is much larger if the VUV pulse is applied at the maximum of the field [time instant (ii), blue lines].

One obvious interpretation of these contributions is a direct double ionization by absorption of a few VUV photons enhanced due to the presence of the IR field. Support for this interpretation is provided by the probability densities taken shortly after the application of the VUV pulse. For example, the probability density in the  $Z$ - $z$  plane (integrated over  $\rho$ ), taken at time instant (i), for application of the VUV at time instant (1), is presented in Fig. 8 (i,1). The comparison with the corresponding density without application of the VUV pulse [Fig. 8 (i,0)] shows the double-ionization signal in the upper and lower triangle of the plot. This corresponds to a

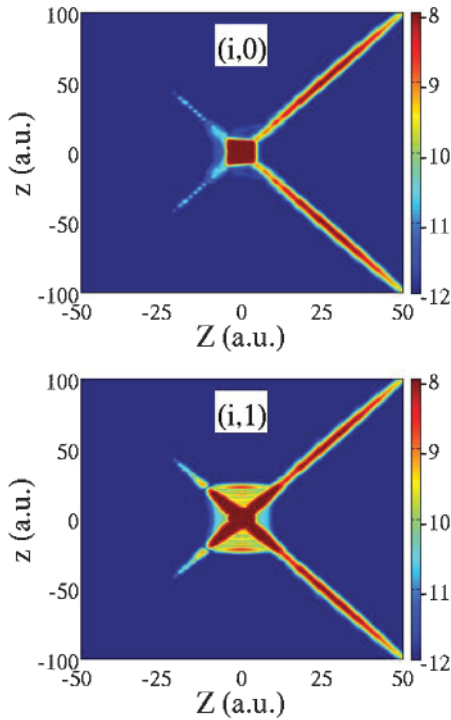


FIG. 8. (Color online) Probability distributions in the  $Z$ - $z$  plane at time instant (i) without (i,0) and with (i,1) application of the VUV pulse at time instant (1) in the presence of the IR pulse.

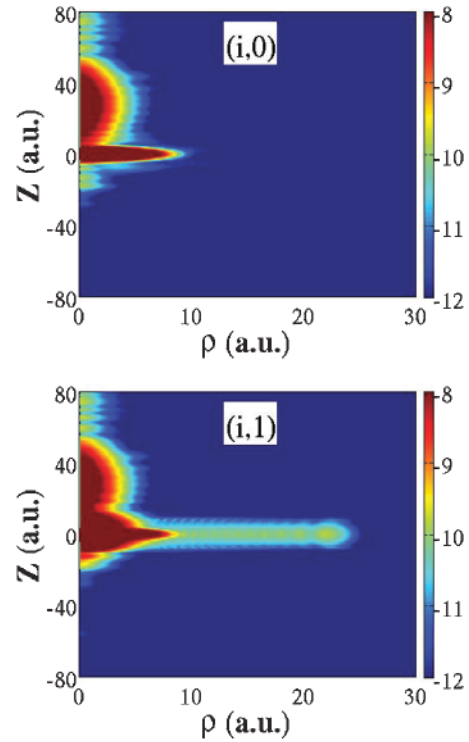


FIG. 9. (Color online) Same as in Fig. 8 but in the  $\rho$ - $Z$  plane.

back-to-back emission of the two electrons, which is known as a signature for a direct double-ionization process in the case of multiphoton absorption due to the strong electron-electron correlation [36]. The strong correlation between the two ejected electrons is also apparent in the corresponding  $\rho$ - $Z$  plot (integrated over  $z$ ), since the additional double-ionization signal due to the VUV pulse appears at large relative distances of the electrons,  $\rho$  (cf. plots without and with application of the VUV pulse in Figs. 9 (i,0) and 9(i,1), respectively).

Please note that a similar feature of a back-to-back emission of the electrons are seen in the  $Z$ - $z$  plot in Figs. 10 (ii,2) and 10(iii,3) for the case of the application of the VUV pulse near the next maximum and the next zero of the IR field [time instants (2) and (3), respectively] as well. In Fig. 10 (ii,2), there is, however, another contribution to double ionization, which appears in the left triangle of the plot. A contribution in this triangle typically indicates a strongly field-driven two-electron process, as in the case of nonsequential double ionization via rescattering (cf., e.g., Ref. [33]). Here it may suggest an enhancement of such a nonsequential process driven by the IR field in the presence of the VUV pulse.

We do observe further increases of the double-ionization signal at subsequent field maxima of the IR pulse (cf. Fig. 7), which are either induced due to the additional single ionization by the VUV pulse or due to excitation of the neutral atom by the VUV pulse followed by direct or nonsequential double ionization from these excited neutral states. Depending on the phase of the IR pulse at which the VUV pulse is applied, the additional single-ionization wave packet can or cannot be driven back to and rescatter with the parent ion. Consequently, we observe that the degree of the enhancement in the

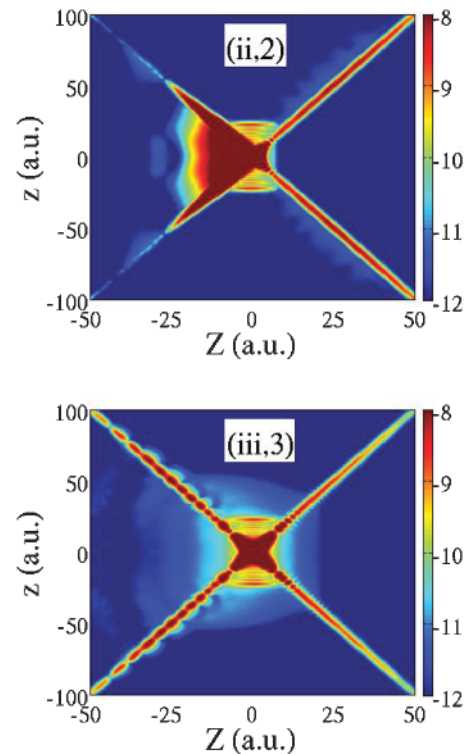


FIG. 10. (Color online) Same as Fig. 8, but for application of the VUV at time instant (2) or (3), and snapshot taken at time instant (ii) or (iii).

double-ionization signal strongly depends on the time delay (phase) at which the VUV pulse is applied.

## VI. CONCLUDING REMARKS

We have investigated the dynamics of a two-electron model of the He atom interacting with an intense near-infrared and an attosecond VUV laser pulse. The parameters of the VUV pulse have been chosen such that ionization from the excited states of the He<sup>+</sup> ion proceed via a one-photon absorption, while absorption of at least two photons are required to ionize the neutral atom or the ion from its ground states. Scenarios, in which the two pulses are applied in sequence or at the same time, have been considered. From the results of our numerical simulations it is found that application of the VUV after the near-infrared pulse does not lead to an enhancement of the double-ionization signal, which let us conclude that there is not significant population in the excited ionic states at the end of the IR pulse at present IR laser parameters. On the other hand, we observe a strong enhancement of the double-ionization

signal if the VUV pulse is either applied before or during the IR pulse. We attribute this to a pumping of excited states in the neutral atom by the VUV pulse, which lead to nonsequential double ionization from these excited states driven by the IR pulse. Regarding the question if attosecond pulse technology can be used to probe certain mechanisms of nonsequential double ionization, in particular the so-called RESI process, our results show that it may be difficult to distinguish processes initiated by the attosecond VUV pulse from those solely driven by the IR pulse in the setups considered in the present work. Such a distinction may be easier if the polarization directions of the two pulses are chosen to be perpendicular in an experiment. This scenario can, however, not be studied using the present two-electron model, since the center-of-mass motion of the two electrons is restricted to one dimension.

## ACKNOWLEDGMENT

This work was supported by NSF.

- 
- [1] F. Krausz and M. Ivanov, *Rev. Mod. Phys.* **81**, 163 (2009).  
 [2] P. B. Corkum and F. Krausz, *Nat. Phys.* **2**, 781 (2007).  
 [3] H. Hasegawa, E. J. Takahashi, Y. Nabekawa, K. L. Ishikawa, and K. Midorikawa, *Phys. Rev. A* **71**, 023407 (2005).  
 [4] P. Antoine, E. Fomouo, B. Piraux, T. Shimizu, H. Hasegawa, Y. Nabekawa, and K. Midorikawa, *Phys. Rev. A* **78**, 023415 (2008).  
 [5] R. Moshhammer *et al.*, *Phys. Rev. Lett.* **98**, 203001 (2007).  
 [6] A. Rudenko *et al.*, *Phys. Rev. Lett.* **101**, 073003 (2008).  
 [7] J. Colgan and M. S. Pindzola, *Phys. Rev. Lett.* **88**, 173002 (2002).  
 [8] S. Laulan and H. Bachau, *Phys. Rev. A* **68**, 013409 (2003).  
 [9] K. L. Ishikawa and K. Midorikawa, *Phys. Rev. A* **72**, 013407 (2005).  
 [10] E. Fomouo, G. L. Kamta, G. Edah, and B. Piraux, *Phys. Rev. A* **74**, 063409 (2006).  
 [11] D. A. Horner, F. Morales, T. N. Rescigno, F. Martín, and C. W. McCurdy, *Phys. Rev. A* **76**, 030701(R) (2007).  
 [12] I. A. Ivanov and A. S. Kheifets, *Phys. Rev. A* **75**, 033411 (2007).  
 [13] L. A. A. Nikolopoulos and P. Lambropoulos, *J. Phys. B: At. Mol. Opt. Phys.* **40**, 1347 (2007).  
 [14] E. Fomouo, P. Antoine, B. Piraux, L. Malegat, H. Bauchau, and R. Shakeshaft, *J. Phys. B: At. Mol. Opt. Phys.* **41**, 051001 (2008).  
 [15] J. Feist, S. Nagele, R. Pazourek, E. Persson, B. I. Schneider, L. A. Collins, and J. Burgdörfer, *Phys. Rev. A* **77**, 043420 (2008).  
 [16] X. Guan, K. Bartschat, and B. I. Schneider, *Phys. Rev. A* **77**, 043421 (2008).  
 [17] J. Feist, S. Nagele, R. Pazourek, E. Persson, B. I. Schneider, L. A. Collins, and J. Burgdörfer, *Phys. Rev. Lett.* **103**, 063002 (2009).  
 [18] A. Palacios, T. N. Rescigno, and C. W. McCurdy, *Phys. Rev. Lett.* **103**, 253001 (2009).  
 [19] M. Uiberacker *et al.* *Nature (London)* **446**, 627 (2007).  
 [20] A. LHuillier, L. A. Lompre, G. Mainfray, and C. Manus, *Phys. Rev. Lett.* **48**, 1814 (1982).  
 [21] B. Walker, B. Sheehy, L. F. DiMauro, P. Agostini, K. J. Schafer, and K. C. Kulander, *Phys. Rev. Lett.* **73**, 1227 (1994).  
 [22] A. Becker, R. Dörner, and R. Moshhammer, *J. Phys. B* **38**, S753 (2005).  
 [23] P. B. Corkum, *Phys. Rev. Lett.* **71**, 1994 (1993).  
 [24] K. J. Schafer, B. Yang, L. F. DiMauro, and K. C. Kulander, *Phys. Rev. Lett.* **70**, 1599 (1993).  
 [25] A similar mechanism, originally named antenna mechanism [26], has been proposed by M. Yu. Kuchiev [27].  
 [26] M. Yu. Kuchiev, *JETP Lett.* **45**, 404 (1987).  
 [27] M. Yu. Kuchiev, *J. Phys. B* **28**, 5093 (1995).  
 [28] K. J. LaGattuta and J. S. Cohen, *J. Phys. B* **31**, 5281 (1998).  
 [29] R. Kopold, W. Becker, H. Rottke, and W. Sandner, *Phys. Rev. Lett.* **85**, 3781 (2000).  
 [30] B. Feuerstein *et al.* *Phys. Rev. Lett.* **87**, 043003 (2001).  
 [31] S. Baier, C. Ruiz, L. Plaja, and A. Becker, *Phys. Rev. A* **74**, 033405 (2006).  
 [32] S. Baier, A. Becker, and L. Plaja, *Phys. Rev. A* **78**, 013409 (2008).  
 [33] C. Ruiz, L. Plaja, L. Roso, and A. Becker, *Phys. Rev. Lett.* **96**, 053001 (2006).  
 [34] C. Ruiz and A. Becker, *New J. Phys.* **10**, 025020 (2008).  
 [35] NIST Atomic Spectra Database [<http://www.nist.gov/physlab/data/asd.cfm>].  
 [36] A. Becker and F. H. M. Faisal, *Phys. Rev. A* **50**, 3256 (1994).